Multipath Interference Compensation in Time-of-Flight Camera Images

Stefan Fuchs
German Aerospace Center
Institute of Robotics and Mechatronics
Oberpfaffenhofen, Germany
stefan.fuchs@dlr.de

Abstract—**Multipath interference is inherent to the working principle of a Time-of-flight camera and can influence the measurements by several centimeters. Especially in applications that demand for high accuracy, such as object localization for robotic manipulation or ego-motion estimation of mobile robots, multipath interference is not tolerable. In this paper we formulate a multipath model in order to estimate the interference and correct the measurements. The proposed approach comprises the measured scene structure. All distracting surfaces are assumed to be Lambertian radiators and the directional interference is simulated for correction purposes. The positive impact of these corrections is experimentally demonstrated.**

Keywords-**time-of-flight camera; range imaging; calibration**

I. Introduction

A **T**ime-**O**f-**f**light (ToF) camera is an active sensor, which basically operates like common CCD or CMOS cameras. The ToF camera emits sinusoidal modulated **N**ear-**I**nfra**R**ed (NIR) light. The NIR light is reflected by the observed scene and the camera optics projects the light onto a CMOS or CMOS/CCD pixel matrix. By means of sophisticated electronics, distances and intensities are computed within every pixel. Thus, the ToF camera provides range and intensity images at high frame rates independent of textures or illumination. Due to the small-sized and handy design, ToF sensors are a good alternative to laser-scanners or stereo camera systems.

ToF cameras are not widespread yet, despite their suitability for a wide range of applications that require 2D/3D information, such as object detection and localization, surveillance tasks or collision avoidance in mobile robotics. The reason is primarily the complex error characteristic of the ToF camera.

II. Related Work

Besides the known intrinsic systematic errors coming from the camera optics, e.g. lens distortion, there are several ToF camera specific errors. First of all, ToF cameras are affected by the distance- and amplitude related errors plus the **F**ixed-**P**attern-**P**hase **N**oise (FPPN). Numerous papers already addressed these issues. In [5], [3], [1] and [2] models of these errors are formulated and calibration procedures are described in order to compensate the systematic ToF camera errors.

Another error source specific to ToF cameras is **M**ulti**P**ath **I**nterference (MPI). Contrary to the theoretical assumptions, the received NIR beam does not exclusively transport the distance information of a certain scene point. Depending on the environment the received signal is superimposed with beams that were reflected multiple times. Such reflections originate either from the camera optics or from the scene.

In the former case, the effect is called light scattering. Light scattering is primarily caused in low quality optics by close and highly reflective objects, whereas the background has a low reflectivity. Thereby, the distance information of the bright and close object is scattered over the whole image. The background seems to be closer to the camera by several decimeters. Mure-Dubois et al. [7] propose a scattering compensation procedure. They describe a space invariant point spread function as a model for the scattering and reduce up to 95% of the scattering effects. Since the assumed position independence of the scattering is not given, these results hold only for simple structured scenes.

MPI also arises from multiple reflections within the scene. This effect is already known from radar processing where it causes ghost targets or from sonar-based range sensors. MPI is hard to predict, since it depends on the scene configuration which is measured. In radar processing a known map of the environment is incorporated in order to eliminate echoes that originate below ground or above a certain height. Recent sonar-based localization algorithms increase the robustness against multipath interference by probabilistic approaches, but do not improve the accuracy.

Gudmundsson [4] experimentally shows the impact of MPI using the example of a corner. Due to the MPI the corner is represented completely inaccurate and the actual orthogonal planes opened up to about $120°$. May et al. demonstrate the MPI in a robotic setting [6]. A ToF camera, attached to a robot, is used for estimating the robot's ego-motion and accumulating a 3D map. They experimentally showed the MPI's dependence on the configuration and reflectivity of the scene. By removing reflecting objects or reducing their reflectivity the ego motion results improved by 50%.

So far, there are some approaches only mitigating the impact of MPI for range sensors similar to ToF cameras. In this paper we will correct the MPI in ToF camera measurements.

Therefor, we pick up the results of [4] and [6]. We refer to the scattering model of [4] and formulate an enhanced multipath model, which incorporates the scene configuration. This model allows for effective correcting of the distance measurements. The positive impact of such a compensation is demonstrated in an ego-motion experiment similar to [6].

III. MODEL OF MULTIPATH INTERFERENCE

In the following the working principle of a ToF camera is outlined and the proposed MPI model is formulated step-by-step according to Figure 1, which sketches an exemplary scene configuration.
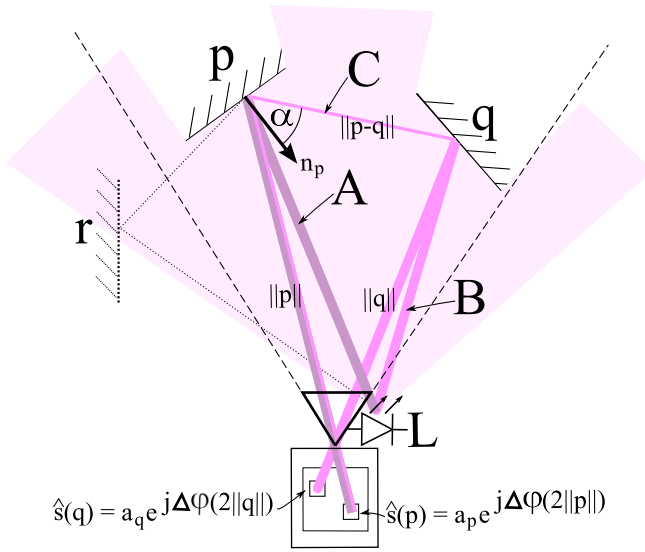
A. Working Principle

Figure 1. Directional multipath interference. The Lambertian emitter L illuminates the whole scene. The sketch focuses on two beams out of the luster cone. Beam A shines on **p** and beam B shines on **q**. If the luster cone is not congruent with the camera's field of view (dashed line), the unseen surface **r** also influences the measurement (dotted line).

In Figure 1, the Lambertian emitter L illuminates the scene with sinusoidal modulated NIR light. Ideally, the beam A goes straight from L to the observed surface at point **p**. The light is reflected there and comes back to the receiver. The received signal $s_{\mathbf{p}}(t)$

$$s_{\mathbf{p}}(t) = h + a_{\mathbf{p}}^{in} \cos(\omega t + \Delta\phi(2\|\mathbf{p}\|))$$

is characterized by three parameters: phase shift $\Delta\phi(2\|\mathbf{p}\|)$, amplitude $a_{\mathbf{p}}^{in}$ and intensity h. The phase shift $\Delta\phi(2\|\mathbf{p}\|)$ is proportional to the covered distance. Given the speed of light c the distance $\|\mathbf{p}\|$ is

$$\|\mathbf{p}\| = \frac{\Delta\phi(2\|\mathbf{p}\|)c}{4\pi} \quad . \tag{1}$$

The amplitude $a_{\mathbf{p}}^{in}$ and the intensity h represent the irradiance. $a_{\mathbf{p}}^{in}$ is the signal strength of the received signal. It is proportional to the reflectivity and inversely proportional

to the squared distance of **p**. The intensity h indicates the constant part of the received signal, i.e. the background illumination. Current available ToF cameras feature background illumination and we can neglect h. Then, we can define the characteristics of the incident light $s(t)$ from **p** in complex notation with

$$s(\mathbf{p}) = a_{\mathbf{p}}^{in} e^{j\Delta\phi(2\|\mathbf{p}\|)} \quad . \tag{2}$$

The complex notation considers the working principle of ToF cameras when describing the superposition of received distance information, which is basically the addition of phasors.

B. Directional Multipath Interference

Figure 1 displays a second beam B, which irradiates the surface at point **q**. We assume **q** to be a Lambertian emitter. Hence, **q** reflects incident light to **p**, as illustrated by the thinner beam C. So, beam B contributes via **q**

$$s(\mathbf{q})^{+} = a_{\mathbf{q}}^{+} e^{j\Delta\phi(\|\mathbf{p}\|+\|\mathbf{q}\|+\|\mathbf{q}-\mathbf{p}\|)} \tag{3}$$

to $s(\mathbf{p})$. As a result, the measured total irradiance $\hat{s}(\mathbf{p})$ is a composition of

$$\hat{s}(\mathbf{p}) = s(\mathbf{p}) + s(\mathbf{q})^{+} \quad . \tag{4}$$

The amplitude $a_{\mathbf{q}}^{+}$ regulates the influence of the additional part $s(\mathbf{q})^{+}$ on $s(\mathbf{p})$. The magnitude of $a_{\mathbf{q}}^{+}$ is linked to the distances of **p**, **q** and their amplitudes. Since the incident amplitude $a_{\mathbf{q}}^{in}$ is inversely proportional to the squared distance, we can compute the light strength and radiance $a_{\mathbf{q}}^{ex}$ of beam C when it is transmitted from **q** with

$$a_{\mathbf{q}}^{ex} = \|\mathbf{q}\|^{2} a_{\mathbf{q}}^{in} \quad . \tag{5}$$

Because of the covered distance $\|\mathbf{p} - \mathbf{q}\|$ and because of the angle α between the normal $\mathbf{n_p}$ and the incident beam C

$$\cos(\alpha) = \frac{(\mathbf{p} - \mathbf{q})}{\|\mathbf{p} - \mathbf{q}\|} \mathbf{n_p}' \tag{6}$$

the incoming signal strength and irradiance $a_{C,\mathbf{q}}^{in}$ of beam C at **p** is

$$a_{C,\mathbf{q}}^{in} = \cos(\alpha) \frac{1}{\|\mathbf{p} - \mathbf{q}\|^{2}} \|\mathbf{q}\|^{2} a_{\mathbf{q}}^{in} \quad . \tag{7}$$

Finally, the last distance from **p** to the camera is incorporated. So the overall amplitude of the additional part is

$$a_{\mathbf{q}}^{+} = \frac{1}{\|\mathbf{p}\|^{2}} \cos(\alpha) \frac{1}{\|\mathbf{p} - \mathbf{q}\|^{2}} \|\mathbf{q}\|^{2} a_{\mathbf{q}}^{in} \quad . \tag{8}$$

From equation 4 the undistorted signal $s(\mathbf{p})$ is

$$s(\mathbf{p}) = \hat{s}(\mathbf{p}) - s(\mathbf{q})^{+} \quad . \tag{9}$$

In fact, the accurate distances and amplitudes of **p**, **q** are required for these computations. Within the scope of the investigations it was discovered, that the searched MPI is significantly smaller than the sum of the influencing additional distances $\|\mathbf{p}\|$, $\|\mathbf{q}\|$ and $\|\mathbf{p} - \mathbf{q}\|$. On this account, the requirements mentioned before are neglected, and we use the measured distances and amplitudes.

C. Accumulated Multipath Interference

Relating to the point of view in $\mathbf{p}$, the surface $\mathbf{p}$ is irradiated by nearly all visible points in the environment - not only once but multiple times. The set Q of these influencing surface points is thus unlimited. Hence, we introduce a second simplification. Due to efficiency considerations the design of the luster cone ideally is congruent with the camera's field of view. If we exclusively consider directional multipath interference, only directly illuminated surfaces influence the measurements. Consequently, Q is limited by the camera's field of view. The measured distance image is transformed into a point cloud with corresponding normals. Thereafter, the set Q for a certain pixel and $\mathbf{p}$ respectively is determined. The MPI-related error for this pixel is the sum of all single contributing parts, which is subtracted from the measurement

$$s(\mathbf{p}) = \hat{s}(\mathbf{p}) - \sum_{\mathbf{q} \in Q} s(\mathbf{q})^+ \quad . \qquad (10)$$

in order to compensate the MPI-related error. This is done for all pixels in the image by using the measured distances and amplitudes.

IV. EXPERIMENTS AND RESULTS

The performance of the proposed MPI compensation method was investigated with an IFM ToF camera[1] in two experiments. This camera features a resolution of 200×200 pixels and an apex angle of $55\,°$. The MPI simulations were done off line in MATLAB and required 10 minutes per image.
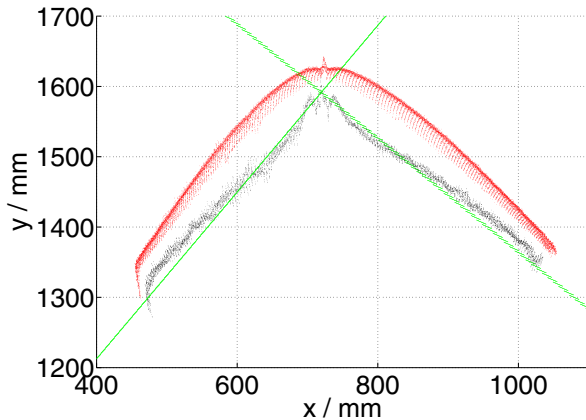
Figure 2. Bird's eye view of the corner located $1\,\mathrm{m}$ in front of the camera. The green points are measured with a laser scanner system. The red points are captured with the ToF camera and affected by MPI. By applying MPI compensation the root mean squared error is reduced from $57\,\mathrm{mm}$ to $17\,\mathrm{mm}$ (black).

First, the impact of MPI was measured in a corner scene (see Figure 2). A laser scanner system provided the Ground
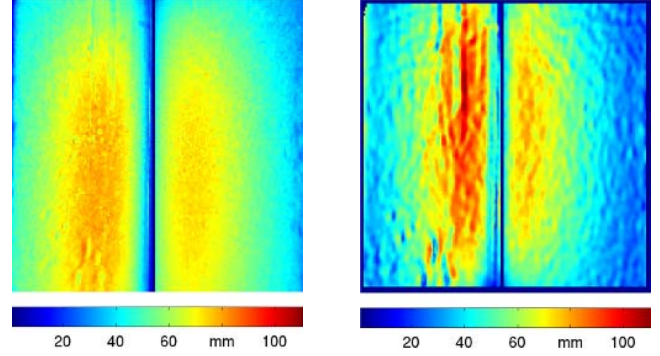
Figure 3. The left diagram illustrates the measured MPI related error in a corner scene. The right image presents the computed MPI. The distributions are similar to a spot. The diagrams do not match perfectly. The spots in the left diagram are stretched more vertically due to the reflections at the floor.

Truth. Figure 3 shows the measured and the simulated MPI. They do not perfectly match, due to the simplifications. The corner is no perfect Lambertian emitter. Thus, the MPI is distributed unbalanced. Furthermore, reflections of unseen surfaces are not considered. The emitted NIR light is partially reflected by the floor and the measured MPI is more stretched to the lower image boundary.

Second, an ego-motion experiment demonstrates the effect of the MPI compensation in a robotic context. The ToF camera was mounted on an industrial robot and moved along two trajectories while capturing a simple scene configuration (see Figure 4). The ToF camera's ego-motion was estimated by applying an ICP algorithm. Further information is given in [6].

The accumulated ego-motion estimation was compared to the robot's trajectory. For both trajectories T_A and T_B the rotational error decreases by applying MPI compensation: In T_A from $5.2\,°$ to $3.4\,°$ and in T_B from $2.3\,°$ to $0.3\,°$. The translational error is reduced only marginally in T_A from $46.9\,\mathrm{mm}$ to $44.3\,\mathrm{mm}$. In contrast, in T_B it is reduced by $50\,\%$ from $137.7\,\mathrm{mm}$ to $55.8\,\mathrm{mm}$ (see Figure 5). However, compared with the total travel distance the localization error in T_B is larger than in T_A. Most likely, the luster cone of the camera is not congruent with the camera's field of view. Thus, the impact of the MPI varies with the trajectory resulting from reflections beyond the camera's field of view.

V. CONCLUSION

This paper discusses multipath interference (MPI) in ToF camera images. MPI distorts the measurements by several centimeters and is thus critical for applications that depend on high accuracy, e.g localization for robotic manipulation. This paper formulates a model of MPI in order to simulate and compensate them. The effective improvements are demonstrated by two experiments.

Basically, there are two issues deserving closer attention. First, the method relies on measured but already distorted
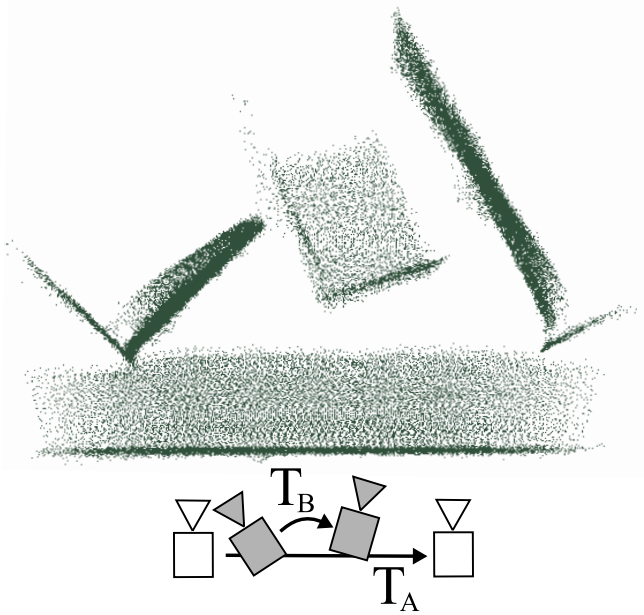
Figure 4. Bird's eye view of the the experimental setup and the measured point cloud. The scene consists of several Styrofoam cuboids. The focus was put on the MPI compensation for a translation T_A (400 mm) and a combined rotation and translation T_B (50 °,150 mm) of the ToF camera.
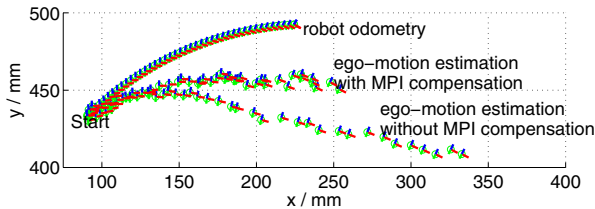

Figure 5. The measured and estimated trajectories of T_B are plotted. The robot positioning system provides odometry data with an accuracy of $1\ mm$ and $0.1°$. The ego-motion estimation without MPI compensation shows a large deviation. The localization error is reduced by the MPI compensation.

distances and amplitudes. Possibly, iterative algorithms can fix this simplification. Second, the compensation method is computationally intensive and does not allow for dynamic applications (in contradiction to ToF cameras). The MPI compensation is similar to rendering and shading tasks. In order to accelerate the computations future investigations will engage in an implementation of the algorithm on a graphics adapter.

References

[1] C. Beder and R. Koch. Calibration of focal length and 3d pose based on the reflectance and depth image of a planar object. In *Proceedings of the DAGM Dyn3D Workshop, Heidelberg, Germany*, volume I, September 2007.

[2] S. Fuchs and G. Hirzinger. Extrinsic and depth calibration of tof-cameras. In *IEEE Conference on Computer Vision and Pattern Recognition (CVPR), Anchorage, USA*, June 2008.

[3] S. Fuchs and S. May. Calibration and registration for precise surface reconstruction. In *Proceedings of the DAGM Dyn3D Workshop, Heidelberg, Germany*, volume I, September 2007.

[4] S. A. Gudmundsson. Environmental effects on measurement uncertainties of time-of-flight cameras. In *Proceedings of the International Symposium on Signals Circuits and Systems - ISSCS*, July 2007.

[5] M. Lindner and A. Kolb. Lateral and depth calibration of pmd-distance sensors. In *In Procedings of the ISVC, Lake Tahoe, USA*, pages 524–533, 2006.

[6] S. May, S. Fuchs, D. Droeschel, D. Holz, and A. Nüchter. Robust 3D-Mapping with Time-of-Flight Cameras. In *Proceedings of the IEEE/RSJ International Conference on Intelligent Robots and Systems (IROS)*, pages 1673–1678, St. Louis, Missouri, USA, October 2009.

[7] J. Mure-Dubois and H. Huegli. Real-time scattering compensation for time-of-flight camera. In *Proceedings of the ICVS Workshop on Camera Calibration Methods for Computer Vision Systems*, 2007.